

# Gilbert damping in two-dimensional metallic anti-ferromagnets

R. J. Sokolewicz,<sup>1,2</sup> M. Baglai,<sup>3</sup> I. A. Ado,<sup>1</sup> M. I. Katsnelson,<sup>1</sup> and M. Titov<sup>1</sup>

<sup>1</sup>*Radboud University, Institute for Molecules and Materials, 6525 AJ Nijmegen, the Netherlands*

<sup>2</sup>*Qblox, Delftechpark 22, 2628 XH Delft, the Netherlands*

<sup>3</sup>*Department of Physics and Astronomy, Uppsala University, Box 516, SE-751 20, Uppsala, Sweden*

(Dated: March 29, 2024)

A finite spin life-time of conduction electrons may dominate Gilbert damping of two-dimensional metallic anti-ferromagnets or anti-ferromagnet/metal heterostructures. We investigate the Gilbert damping tensor for a typical low-energy model of a metallic anti-ferromagnet system with honeycomb magnetic lattice and Rashba spin-orbit coupling for conduction electrons. We distinguish three regimes of spin relaxation: exchange-dominated relaxation for weak spin-orbit coupling strength, Elliot-Yafet relaxation for moderate spin-orbit coupling, and Dyakonov-Perel relaxation for strong spin-orbit coupling. We show, however, that the latter regime takes place only for the in-plane Gilbert damping component. We also show that anisotropy of Gilbert damping persists for any finite spin-orbit interaction strength provided we consider no spatial variation of the Néel vector. Isotropic Gilbert damping is restored only if the electron spin-orbit length is larger than the magnon wavelength. Our theory applies to MnPS<sub>3</sub> monolayer on Pt or to similar systems.

## I. INTRODUCTION

Magnetization dynamics in anti-ferromagnets continue to attract a lot of attention in the context of possible applications<sup>1–4</sup>. Various proposals utilize the possibility of THz frequency switching of anti-ferromagnetic domains for ultrafast information storage and computation<sup>5,6</sup>. The rise of van der Waals magnets has had a further impact on the field due to the possibility of creating tunable heterostructures that involve anti-ferromagnet and semiconducting layers<sup>7</sup>.

Understanding relaxation of both the Néel vector and non-equilibrium magnetization in anti-ferromagnets is recognized to be of great importance for the functionality of spintronic devices<sup>8–13</sup>. On one hand, low Gilbert damping must generally lead to better electric control of magnetic order via domain wall motion or ultrafast domain switching<sup>14–16</sup>. On the other hand, an efficient control of magnetic domains must generally require a strong coupling between charge and spin degrees of freedom due to a strong spin-orbit interaction, that is widely thought to be equivalent to strong Gilbert damping.

In this paper, we focus on a microscopic analysis of Gilbert damping due to Dyakonov-Perel and Elliot-Yafet mechanisms. We apply the theory to a model of a two-dimensional Néel anti-ferromagnet with a honeycomb magnetic lattice.

Two-dimensional magnets typically exhibit either easy-plane or easy-axis anisotropy, and play crucial roles in stabilizing magnetism at finite temperatures<sup>17,18</sup>. Easy-axis anisotropy selects a specific direction for magnetization, thereby defining an axis for the magnetic order. In contrast, easy-plane anisotropy does not select a particular in-plane direction for the Néel vector, allowing it to freely rotate within the plane. This situation is analogous to the XY model, where the system's continuous symmetry leads to the suppression of out-of-plane fluctuations rather than fixing the magnetization in a specific in-plane direction<sup>19,20</sup>. Without this anisotropy, the

magnonic fluctuations in a two-dimensional crystal can grow uncontrollably large to destroy any long-range magnetic order, according to the Mermin-Wagner theorem<sup>21</sup>.

Recent density-functional-theory calculations for single-layer transition metal trichalcogenides<sup>22</sup>, predict the existence of a large number of metallic anti-ferromagnets with honeycomb lattice and different types of magnetic order as shown in Fig. 1. Many of these crystals may have the Néel magnetic order as shown in Fig. 1a and are metallic: FeSiSe<sub>3</sub>, FeSiTe<sub>3</sub>, VGeTe<sub>3</sub>, MnGeS<sub>3</sub>, FeGeSe<sub>3</sub>, FeGeTe<sub>3</sub>, NiGeSe<sub>3</sub>, MnSnS<sub>3</sub>, MnSnS<sub>3</sub>, MnSnSe<sub>3</sub>, FeSnSe<sub>3</sub>, NiSnS<sub>3</sub>. Apart from that it has been predicted that anti-ferromagnetism can be induced in graphene by bringing it in proximity to MnPSe<sub>3</sub><sup>23</sup> or by bringing it in double proximity between a layer of Cr<sub>2</sub>Ge<sub>2</sub>Te<sub>6</sub> and WS<sub>2</sub><sup>24</sup>.

Partly inspired by these predictions and recent technological advances in producing single-layer anti-ferromagnet crystals, we propose an effective model to study spin relaxation in 2D honeycomb anti-ferromagnet with Néel magnetic order. The same system was studied by us in Ref. 25, where we found that spin-orbit coupling introduces a weak anisotropy in spin-orbit torque and electric conductivity. Strong spin-orbit coupling was shown to lead to a giant anisotropy of Gilbert damping.

Our analysis below is built upon the results of Ref. 25, and we investigate and identify three separate regimes of spin-orbit strength. Each regime is characterized by qualitatively different dependence of Gilbert damping on spin-orbit interaction and conduction electron transport time. The regime of weak spin-orbit interaction is dominated by exchange field relaxation of electron spin, and the regime of moderate spin-orbit strength is dominated by Elliot-Yafet spin relaxation. These two regimes are characterized also by a universal factor of 2 anisotropy of Gilbert damping. The regime of strong spin-orbit strength, which leads to substantial splitting of electron Fermi surfaces, is characterized by Dyakonov-Perel relaxation of the in-plane spin component and Elliot-Yafet re-

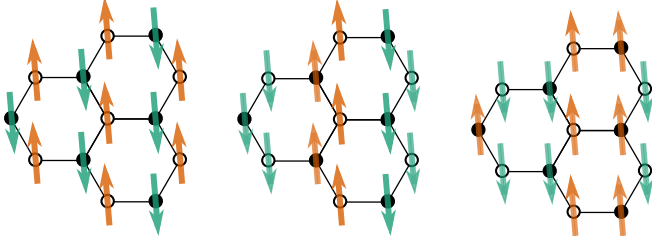


FIG. 1. Three anti-ferromagnetic phases commonly found among van-der-Waals magnets. Left-to-right: Néel, zig-zag, and stripy.

laxation of the perpendicular-to-the-plane Gilbert damping which leads to a giant damping anisotropy. Isotropic Gilbert damping is restored only for finite magnon wave vectors such that the magnon wavelength is smaller than the spin-orbit length.

Gilbert damping in a metallic anti-ferromagnet can be qualitatively understood in terms of the Fermi surface breathing<sup>26</sup>. A change in the magnetization direction gives rise to a change in the Fermi surface to which the conduction electrons have to adjust. This electronic re-configuration is achieved through the scattering of electrons off impurities, during which angular momentum is transferred to the lattice. Gilbert damping, then, should be proportional to both (i) the ratio of the spin life-time and momentum life-time of conduction electrons, and (ii) the electric conductivity. Keeping in mind that the conductivity itself is proportional to momentum life-time, one may conclude that the Gilbert damping is linearly proportional to the spin life-time of conduction electrons. At the same time, the spin life-time of localized spins is *inversely* proportional to the spin life-time of conduction electrons. A similar relation between the spin life-times of conduction and localized electrons also holds for relaxation mechanisms that involve electron-magnon scattering<sup>27</sup>.

Our approach formally decomposes the magnetic system into a classical sub-system of localized magnetic moments and a quasi-classical subsystem of conduction electrons. A local magnetic exchange couples these sub-systems. Localized magnetic moments in transition-metal chalcogenides and halides form a hexagonal lattice. Here we focus on the Néel type anti-ferromagnet that is illustrated in Fig. 1a. In this case, one can define two sub-lattices A and B that host local magnetic moments  $\mathbf{S}^A$  and  $\mathbf{S}^B$ , respectively. For the discussion of Gilbert damping, we ignore the weak dependence of both fields on atomic positions and assume that the modulus  $S = |\mathbf{S}^{A(B)}|$  is time-independent.

Under these assumptions, the magnetization dynamics of localized moments may be described in terms of two fields

$$\mathbf{m} = \frac{1}{2S}(\mathbf{S}^A + \mathbf{S}^B), \quad \mathbf{n} = \frac{1}{2S}(\mathbf{S}^A - \mathbf{S}^B), \quad (1)$$

which are referred to as the magnetization and staggered

magnetization (or Néel vector), respectively. Within the mean-field approach, the vector fields yield the equations of motion

$$\dot{\mathbf{n}} = -J \mathbf{n} \times \mathbf{m} + \mathbf{n} \times \delta \mathbf{s}^+ + \mathbf{m} \times \delta \mathbf{s}^-, \quad (2a)$$

$$\dot{\mathbf{m}} = \mathbf{m} \times \delta \mathbf{s}^+ + \mathbf{n} \times \delta \mathbf{s}^-, \quad (2b)$$

where dot stands for the time derivative, while  $\delta \mathbf{s}^+$  and  $\delta \mathbf{s}^-$  stand for the mean staggered and non-staggered non-equilibrium fields that are proportional to the variation of the corresponding spin-densities of conduction electrons caused by the time dynamics of  $\mathbf{n}$  and  $\mathbf{m}$  fields. The energy  $J$  is proportional to the anti-ferromagnet exchange energy for localized momenta.

In Eqs. (2) we have omitted terms that are proportional to easy axis anisotropy for the sake of compactness. These terms are, however, important and will be introduced later in the text.

In the framework of Eqs. (2) the Gilbert damping can be computed as the linear response of the electron spin-density variation to a time change in both the magnetization and the Néel vector (see e. g. Refs.<sup>25,28,29</sup>).

In this definition, Gilbert damping describes the relaxation of localized spins by transferring both total and staggered angular momenta to the lattice by means of conduction electron scattering off impurities. Such a transfer is facilitated by spin-orbit interaction.

The structure of the full Gilbert damping tensor can be rather complicated as discussed in Ref. 25. However, by taking into account easy axis or easy plane anisotropy we may reduce the complexity of relevant spin configurations to parameterize

$$\delta \mathbf{s}^+ = \alpha_m^{\parallel} \dot{\mathbf{m}}_{\parallel} + \alpha_m^{\perp} \dot{\mathbf{m}}_{\perp} + \alpha_m \mathbf{n}_{\parallel} \times (\mathbf{n}_{\parallel} \times \dot{\mathbf{m}}_{\parallel}), \quad (3a)$$

$$\delta \mathbf{s}^- = \alpha_n^{\parallel} \dot{\mathbf{n}}_{\parallel} + \alpha_n^{\perp} \dot{\mathbf{n}}_{\perp} + \alpha_n \mathbf{n}_{\parallel} \times (\mathbf{n}_{\parallel} \times \dot{\mathbf{n}}_{\parallel}), \quad (3b)$$

where the superscripts  $\parallel$  and  $\perp$  refer to the in-plane and perpendicular-to-the-plane projections of the corresponding vectors, respectively. The six coefficients  $\alpha_m^{\parallel}$ ,  $\alpha_m^{\perp}$ ,  $\alpha_m$ ,  $\alpha_n^{\parallel}$ ,  $\alpha_n^{\perp}$ , and  $\alpha_n$  parameterize the Gilbert damping.

Inserting Eqs. (3) into the equations of motion of Eqs. (2) produces familiar Gilbert damping terms. The damping proportional to time-derivatives of the Néel vector  $\mathbf{n}$  is in general many orders of magnitude smaller than that proportional to the time-derivatives of the magnetization vector  $\mathbf{m}$ <sup>25,30</sup>. Due to the same reason, the higher harmonics term  $\alpha_m \mathbf{n}_{\parallel} \times (\mathbf{n}_{\parallel} \times \partial_t \mathbf{m}_{\parallel})$  can often be neglected.

Thus, in the discussion below we may focus mostly on the coefficients  $\alpha_m^{\parallel}$  and  $\alpha_m^{\perp}$  that play the most important role in the magnetization dynamics of our system. The terms proportional to the time-derivative of  $\mathbf{n}$  correspond to the transfer of angular momentum between the sub-lattices and are usually less relevant. We refer to the results of Ref. 25 when discussing these terms.

All Gilbert damping coefficients are intimately related to the electron spin relaxation time. The latter is relatively well understood in non-magnetic semiconductors

with spin-orbital coupling. When a conducting electron moves in a steep potential it feels an effective magnetic field caused by relativistic effects. Thus, in a disordered system, the electron spin is subject to a random magnetic field each time it scatters off an impurity. At the same time, an electron also experiences precession around an effective spin-orbit field when it moves in between the collisions. Changes in spin direction *between* collisions are referred to as Dyakonov-Perel relaxation<sup>31,32</sup>, while changes in spin-direction *during* collisions are referred to as Elliot-Yafet relaxation<sup>33,34</sup>.

The spin-orbit field in semiconductors induces a characteristic frequency of spin precession  $\Omega_s$ , while scalar disorder leads to a finite transport time  $\tau$  of the conducting electrons. One may, then, distinguish two limits: (i)  $\Omega_s\tau \ll 1$  in which case the electron does not have sufficient time to change its direction between consecutive scattering events (Elliot-Yafet relaxation), and (ii)  $\Omega_s\tau \gg 1$  in which case the electron spin has multiple precession cycles in between the collisions (Dyakonov-Perel relaxation).

The corresponding processes define the so-called spin relaxation time,  $\tau_s$ . In a 2D system the spin life-time  $\tau_s^\parallel$ , for the in-plane spin components, appears to be double the size of the life-time of the spin component that is perpendicular to the plane,  $\tau_s^\perp$ <sup>32</sup>. This geometric effect has largely been overlooked. For non-magnetic 2D semiconductor one can estimate<sup>35,36</sup>

$$\frac{1}{\tau_s^\parallel} \sim \begin{cases} \Omega_s^2\tau, & \Omega_s\tau \ll 1 \\ 1/\tau, & \Omega_s\tau \gg 1 \end{cases}, \quad \tau_s^\parallel = 2\tau_s^\perp. \quad (4)$$

A pedagogical derivation and discussion of Eq. 4 can be found in Refs. 35 and 36. Because electrons are confined in two dimensions the random spin-orbit field is always directed in-plane, which leads to a decrease in the in-plane spin-relaxation rate by a factor of two compared to the out-of-plane spin-relaxation rate as demonstrated first in Ref. 32 (see Refs. 36–40 as well). The reason is that the perpendicular-to-the-plane component of spin is influenced by two components of the randomly changing magnetic field, i.e.  $x$  and  $y$ , whereas the parallel-to-the-plane spin components are only influenced by a single component of the fluctuating fields, i.e. the  $x$  spin projection is influenced only by the  $y$  component of the field and vice-versa. The argument has been further generalized in Ref. 25 to the case of strongly separated spin-orbit split Fermi surfaces. In this limit, the perpendicular-to-the-plane spin-flip processes on scalar disorder potential become fully suppressed. As a result, the perpendicular-to-the-plane spin component becomes nearly conserved, which results in a giant anisotropy of Gilbert damping in this regime.

In magnetic systems that are, at the same time, conducting there appears to be at least one additional energy scale,  $\Delta_{sd}$ , that characterizes exchange coupling of conduction electron spin to the average magnetic moment of localized electrons. (In the case of s-d model description

it is the magnetic exchange between the spin of conduction  $s$  electron and the localized magnetic moment of  $d$  or  $f$  electron on an atom.) This additional energy scale complicates the simple picture of Eq. (4) especially in the case of an anti-ferromagnet. The electron spin precession is now defined not only by spin-orbit field but also by  $\Delta_{sd}$ . As the result the conditions  $\Omega_s\tau \ll 1$  and  $\Delta_{sd}\tau \gg 1$  may easily coexist. This dissolves the distinction between Elliot-Yafet and Dyakonov-Perel mechanisms of spin relaxation. One may, therefore, say that both Elliot-Yafet and Dyakonov-Perel mechanisms may act simultaneously in a typical 2D metallic magnet with spin-orbit coupling. The Gilbert damping computed from the microscopic model that we formulate below will always contain both contributions to spin-relaxation.

## II. MICROSCOPIC MODEL AND RESULTS

The microscopic model that we employ to calculate Gilbert damping is the so-called  $s$ - $d$  model that couples localized magnetic momenta  $\mathbf{S}^A$  and  $\mathbf{S}^B$  and conducting electron spins via the local magnetic exchange  $\Delta_{sd}$ . Our effective low-energy Hamiltonian for conduction electrons reads

$$H = v_f \mathbf{p} \cdot \boldsymbol{\Sigma} + \frac{\lambda}{2} [\boldsymbol{\sigma} \times \boldsymbol{\Sigma}]_z - \Delta_{sd} \mathbf{n} \cdot \boldsymbol{\sigma} \Sigma_z \Lambda_z + V(\mathbf{r}), \quad (5)$$

where the vectors  $\boldsymbol{\Sigma}$ ,  $\boldsymbol{\sigma}$  and  $\boldsymbol{\Lambda}$  denote the vectors of Pauli matrices acting on sub-lattice, spin and valley space, respectively. We also introduce the Fermi velocity  $v_f$ , Rashba-type spin-orbit interaction  $\lambda$ , and a random impurity potential  $V(\mathbf{r})$ .

The Hamiltonian of Eq. (5) can be viewed as the graphene electronic model where conduction electrons have 2D Rashba spin-orbit coupling and are also coupled to anti-ferromagnetically ordered classical spins on the honeycomb lattice.

The coefficients  $\alpha_m^\parallel$  and  $\alpha_m^\perp$  are obtained using linear response theory for the response of spin-density  $\delta \mathbf{s}^+$  to the time-derivative of magnetization vector  $\partial_t \mathbf{m}$ . Impurity potential  $V(\mathbf{r})$  is important for describing momentum relaxation to the lattice. This is related to the angular momentum relaxation due to spin-orbit coupling. The effect of random impurity potential is treated perturbatively in the (diffusive) ladder approximation that involves a summation over diffusion ladder diagrams. The details of the microscopic calculation can be found in the Appendices.

Before presenting the disorder-averaged quantities  $\alpha_m^{\parallel,\perp}$ , it is instructive to consider first the contribution to Gilbert damping originating from a small number of electron-impurity collisions. This clarifies how the number of impurity scattering effects will affect the final result.

Let us annotate the Gilbert damping coefficients with an additional superscript  $(l)$  that denotes the number of scattering events that are taken into account. This

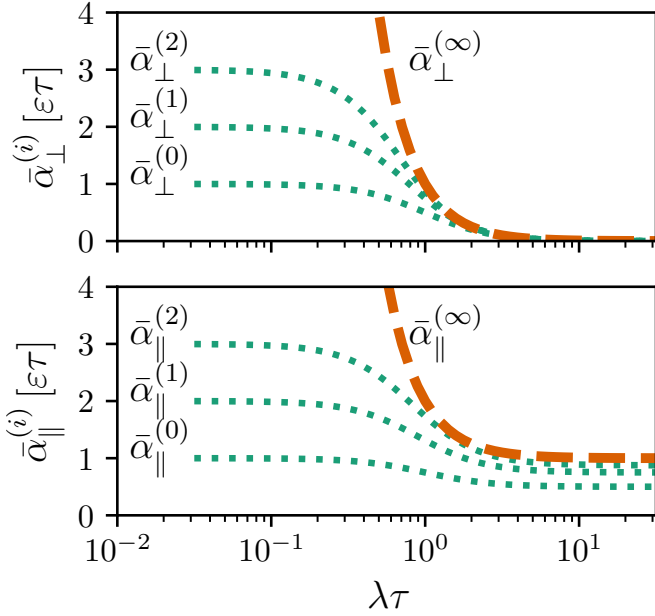


FIG. 2. Gilbert damping in the limit  $\Delta_{sd} = 0$ . Dotted (green) lines correspond to the results of the numerical evaluation of  $\bar{\alpha}_{m,\perp,\parallel}^{(l)}$  for  $l = 0, 1, 2$  as a function of the parameter  $\lambda\tau$ . The dashed (orange) line corresponds to the diffusive (fully vertex corrected) results for  $\bar{\alpha}_{m,\perp,\parallel}^{(\infty)}$ .

means, in the diagrammatic language, that the corresponding quantity is obtained by summing up the ladder diagrams with  $\leq l$  disorder lines. Each disorder line corresponds to a quasi-classical scattering event from a single impurity. The corresponding Gilbert damping coefficient is, therefore, obtained in the approximation where conduction electrons have scattered at most  $l$  number of times before releasing their non-equilibrium magnetic moment into a lattice.

To make final expressions compact we define the dimensionless Gilbert damping coefficients  $\bar{\alpha}_m^{\parallel,\perp}$  by extracting the scaling factor

$$\alpha_m^{\parallel,\perp} = \frac{\mathcal{A}\Delta_{sd}^2}{\pi\hbar^2 v_f^2 S} \bar{\alpha}_m^{\parallel,\perp}, \quad (6)$$

where  $\mathcal{A}$  is the area of the unit cell,  $v_f$  is the Fermi velocity of the conducting electrons and  $\hbar = h/2\pi$  is the Planck's constant. We also express the momentum scattering time  $\tau$  in inverse energy units,  $\tau \rightarrow \hbar\tau$ .

Let us start by computing the coefficients  $\bar{\alpha}_m^{\parallel,\perp(l)}$  in the formal limit  $\Delta_{sd} \rightarrow 0$ . We can start with the “bare bubble” contribution which describes spin relaxation without a single scattering event. The corresponding results read

$$\bar{\alpha}_{m,\perp}^{(0)} = \varepsilon\tau \frac{1 - \lambda^2/4\varepsilon^2}{1 + \lambda^2\tau^2}, \quad (7a)$$

$$\bar{\alpha}_{m,\parallel}^{(0)} = \varepsilon\tau \left( \frac{1 + \lambda^2\tau^2/2}{1 + \lambda^2\tau^2} - \frac{\lambda^2}{8\varepsilon^2} \right), \quad (7b)$$

where  $\varepsilon$  denotes the Fermi energy which we consider positive (electron-doped system).

In all realistic cases, we have to consider  $\lambda/\varepsilon \ll 1$ , while the parameter  $\lambda\tau$  may in principle be arbitrary. For  $\lambda\tau \ll 1$  the disorder-induced broadening of the electron Fermi surfaces exceeds the spin-orbit induced splitting. In this case one basically finds no anisotropy of “bare” damping:  $\bar{\alpha}_{m,\perp}^{(0)} = \bar{\alpha}_{m,\parallel}^{(0)}$ . In the opposite limit of substantial spin-orbit splitting one gets an ultimately anisotropic damping  $\bar{\alpha}_{m,\perp}^{(0)} \ll \bar{\alpha}_{m,\parallel}^{(0)}$ . This asymptotic behavior can be summarized as

$$\bar{\alpha}_{m,\perp}^{(0)} = \varepsilon\tau \begin{cases} 1 & \lambda\tau \ll 1, \\ (\lambda\tau)^{-2} & \lambda\tau \gg 1, \end{cases} \quad (8a)$$

$$\bar{\alpha}_{m,\parallel}^{(0)} = \varepsilon\tau \begin{cases} 1 & \lambda\tau \ll 1, \\ \frac{1}{2}(1 + (\lambda\tau)^{-2}) & \lambda\tau \gg 1, \end{cases} \quad (8b)$$

where we have used that  $\varepsilon \gg \lambda$ .

The results of Eq. (8) modify by electron diffusion. By taking into account up to  $l$  scattering events we obtain

$$\bar{\alpha}_{m,\perp}^{(l)} = \varepsilon\tau \begin{cases} l + \mathcal{O}(\lambda^2\tau^2) & \lambda\tau \ll 1, \\ (1 + \delta_{l0})/(\lambda\tau)^2 & \lambda\tau \gg 1, \end{cases} \quad (9a)$$

$$\bar{\alpha}_{m,\parallel}^{(l)} = \varepsilon\tau \begin{cases} l + \mathcal{O}(\lambda^2\tau^2) & \lambda\tau \ll 1, \\ 1 - (1/2)^{l+1} + \mathcal{O}((\lambda\tau)^{-2}) & \lambda\tau \gg 1, \end{cases} \quad (9b)$$

where we have used  $\varepsilon \gg \lambda$  again.

From Eqs. (9) we see that the Gilbert damping for  $\lambda\tau \ll 1$  gets an additional contribution of  $\varepsilon\tau$  from each scattering event as illustrated numerically in Fig. 2. This leads to a formal divergence of Gilbert damping in the limit  $\lambda\tau \ll 1$ . While, at first glance, the divergence looks like a strong sensitivity of damping to impurity scattering, in reality, it simply reflects a diverging spin life-time. Once a non-equilibrium magnetization  $\mathbf{m}$  is created it becomes almost impossible to relax it to the lattice in the limit of weak spin-orbit coupling. The formal divergence of  $\alpha_m^\perp = \alpha_m^\parallel$  simply reflects the conservation law for electron spin polarization in the absence of spin-orbit coupling such that the corresponding spin life-time becomes arbitrarily large as compared to the momentum scattering time  $\tau$ .

By taking the limit  $l \rightarrow \infty$  (i.e. by summing up the entire diffusion ladder) we obtain compact expressions

$$\bar{\alpha}_m^\perp \equiv \bar{\alpha}_{m,\perp}^{(\infty)} = \varepsilon\tau \frac{1}{2\lambda^2\tau^2}, \quad (10a)$$

$$\bar{\alpha}_m^\parallel \equiv \bar{\alpha}_{m,\parallel}^{(\infty)} = \varepsilon\tau \frac{1 + \lambda^2\tau^2}{\lambda^2\tau^2}, \quad (10b)$$

which assume  $\bar{\alpha}_m^\perp \ll \bar{\alpha}_m^\parallel$  for  $\lambda\tau \gg 1$  and  $\bar{\alpha}_m^\perp = \bar{\alpha}_m^\parallel/2$  for  $\lambda\tau \ll 1$ . The factor of 2 difference that we observe when  $\lambda\tau \ll 1$ , corresponds to a difference in the electron spin life-times  $\tau_s^\perp = \tau_s^\parallel/2$  that was discussed in the introduction<sup>32</sup>.

Strong spin-orbit coupling causes a strong out-of-plane anisotropy of damping,  $\bar{\alpha}_m^\perp \ll \bar{\alpha}_m^\parallel$  which corresponds to

a suppression of the perpendicular-to-the-plane damping component. As a result, the spin-orbit interaction makes it much easier to relax the magnitude of the  $m_z$  component of magnetization than that of in-plane components.

Let us now turn to the dependence of  $\bar{\alpha}_m$  coefficients on  $\Delta_{sd}$  that is illustrated numerically in Fig. 3. We consider first the case of absent spin-orbit coupling  $\lambda = 0$ . In this case, the combination of spin-rotational and sub-lattice symmetry (the equivalence of A and B sub-lattice) must make Gilbert damping isotropic (see e.g.<sup>25,41</sup>). The direct calculation for  $\lambda = 0$  does, indeed, give rise to the isotropic result  $\bar{\alpha}_m^\perp = \bar{\alpha}_m^\parallel = \varepsilon\tau(\varepsilon^2 + \Delta_{sd}^2)/2\Delta_{sd}^2$ , which is, however, in contradiction to the limit  $\lambda \rightarrow 0$  in Eq. (10).

At first glance, this contradiction suggests the existence of a certain energy scale for  $\lambda$  over which the anisotropy emerges. The numerical analysis illustrated in Fig. 4 reveals that this scale does not depend on the values of  $1/\tau$ ,  $\Delta_{sd}$ , or  $\varepsilon$ . Instead, it is defined solely by numerical precision. In other words, an isotropic Gilbert damping is obtained only when the spin-orbit strength  $\lambda$  is set below the numerical precision in our model. We should, therefore, conclude that the transition from isotropic to anisotropic (factor of 2) damping occurs exactly at  $\lambda = 0$ . Interestingly, the factor of 2 anisotropy is absent in Eqs. (8) and emerges only in the diffusive limit.

We will see below that this paradox can only be resolved by analyzing the Gilbert damping beyond the infinite wave-length limit.

One can see from Fig. 3 that the main effect of finite  $\Delta_{sd}$  is the regularization of the Gilbert damping divergence  $(\lambda\tau)^{-2}$  in the limit  $\lambda\tau \ll 1$ . Indeed, the limit of weak spin-orbit coupling is non-perturbative for  $\Delta_{sd}/\varepsilon \ll \lambda\tau \ll 1$ , while, in the opposite limit,  $\lambda\tau \ll \Delta_{sd}/\varepsilon \ll 1$ , the results of Eqs. (10) are no longer valid. Assuming  $\Delta_{sd}/\varepsilon \ll 1$  we obtain the asymptotic expressions for the results presented in Fig. 3 as

$$\bar{\alpha}_m^\perp = \frac{1}{2}\varepsilon\tau \begin{cases} \frac{2}{3} \frac{\varepsilon^2 + \Delta_{sd}^2}{\Delta_{sd}^2} & \lambda\tau \ll \Delta_{sd}/\varepsilon, \\ \frac{1}{\lambda^2\tau^2} & \lambda\tau \gg \Delta_{sd}/\varepsilon, \end{cases} \quad (11a)$$

$$\bar{\alpha}_m^\parallel = \varepsilon\tau \begin{cases} \frac{2}{3} \frac{\varepsilon^2 + \Delta_{sd}^2}{\Delta_{sd}^2} & \lambda\tau \ll \Delta_{sd}/\varepsilon, \\ 1 + \frac{1}{\lambda^2\tau^2} & \lambda\tau \gg \Delta_{sd}/\varepsilon, \end{cases} \quad (11b)$$

which suggest that  $\bar{\alpha}_m^\perp/\bar{\alpha}_m^\parallel = 2$  for  $\lambda\tau \ll 1$ . In the opposite limit,  $\lambda\tau \gg 1$ , the anisotropy of Gilbert damping grows as  $\bar{\alpha}_m^\parallel/\bar{\alpha}_m^\perp = 2\lambda^2\tau^2$ .

The results of Eqs. (11) can also be discussed in terms of the electron spin life-time,  $\tau_s^{\perp(\parallel)} = \bar{\alpha}_m^{\perp(\parallel)}/\varepsilon$ . For the inverse in-plane spin life-time we find

$$\frac{1}{\tau_s^\parallel} = \begin{cases} 3\Delta_{sd}^2/2\varepsilon^2\tau & \lambda\tau \ll \Delta_{sd}/\varepsilon, \\ \lambda^2\tau & \Delta_{sd}/\varepsilon \ll \lambda\tau \ll 1, \\ 1/\tau & 1 \ll \lambda\tau, \end{cases} \quad (12)$$

that, for  $\Delta_{sd} = 0$ , is equivalent to the known result of Eq. (4). Indeed, for  $\Delta_{sd} = 0$ , the magnetic exchange

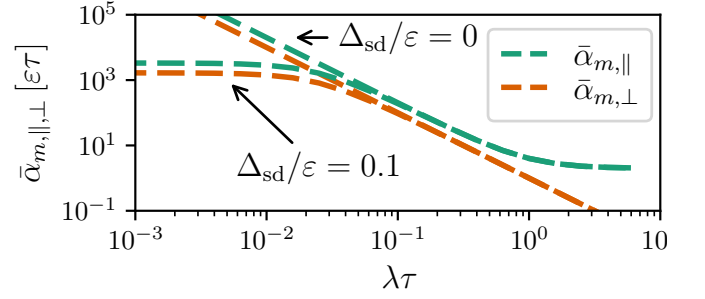


FIG. 3. Numerical results for the Gilbert damping components in the diffusive limit (vertex corrected) as the function of the spin-orbit coupling strength  $\lambda$ . The results correspond to  $\varepsilon\tau = 50$  and  $\Delta_{sd}\tau = 0.1$  and agree with the asymptotic expressions of Eq. (11). Three different regimes can be distinguished for  $\bar{\alpha}_m^\parallel$ : i) spin-orbit independent damping  $\bar{\alpha}_m^\parallel \propto \varepsilon^3\tau/\Delta_{sd}^2$  for the exchange dominated regime,  $\lambda\tau \ll \Delta_{sd}/\varepsilon$ , ii) the damping  $\bar{\alpha}_m^\parallel \propto \varepsilon/\lambda^2\tau$  for Elliot-Yafet relaxation regime,  $\Delta_{sd}/\varepsilon \ll \lambda\tau \ll 1$ , and iii) the damping  $\bar{\alpha}_m^\parallel \propto \varepsilon\tau$  for the Dyakonov-Perel relaxation regime,  $\lambda\tau \gg 1$ . The latter regime is manifestly absent for  $\bar{\alpha}_m^\perp$  in accordance with Eqs. (12,13).

plays no role and one observes the cross-over from Elliot-Yafet ( $\lambda\tau \ll 1$ ) to Dyakonov-Perel ( $\lambda\tau \gg 1$ ) spin relaxation.

This cross-over is, however, absent in the relaxation of the perpendicular spin component

$$\frac{1}{\tau_s^\perp} = 2 \begin{cases} 3\Delta_{sd}^2/2\varepsilon^2\tau & \lambda\tau \ll \Delta_{sd}/\varepsilon, \\ \lambda^2\tau & \Delta_{sd}/\varepsilon \ll \lambda\tau, \end{cases} \quad (13)$$

where Elliot-Yafet-like relaxation extends to the regime  $\lambda\tau \gg 1$ .

As mentioned above, the factor of two anisotropy in spin-relaxation of  $2D$  systems,  $\tau_s^\parallel = 2\tau_s^\perp$ , is known in the literature<sup>32</sup> (see Refs.<sup>36-38</sup> as well). Unlimited growth of spin life-time anisotropy,  $\tau_s^\parallel/\tau_s^\perp = 2\lambda^2\tau^2$ , in the regime  $\lambda\tau \ll 1$  has been described first in Ref. 25. It can be qualitatively explained by a strong suppression of spin-flip processes for  $z$  spin component due to spin-orbit induced splitting of Fermi surfaces. The mechanism is effective only for scalar (non-magnetic) disorder. Even though such a mechanism is general for any magnetic or non-magnetic  $2D$  material with Rashba-type spin-orbit coupling, the effect of the spin life-time anisotropy on Gilbert damping is much more relevant for anti-ferromagnets. Indeed, in an anti-ferromagnetic system the modulus of  $\mathbf{m}$  is, by no means, conserved, hence the variations of perpendicular and parallel components of the magnetization vector are no longer related.

In the regime,  $\lambda\tau \ll \Delta_{sd}/\varepsilon$  the spin life-time is defined by exchange interaction and the distinction between Dyakonov-Perel and Elliot-Yafet mechanisms of spin relaxation is no longer relevant. In this regime, the spin-relaxation time is by a factor  $(\varepsilon/\Delta_{sd})^2$  larger than the momentum relaxation time.

Let us now return to the problem of emergency of the



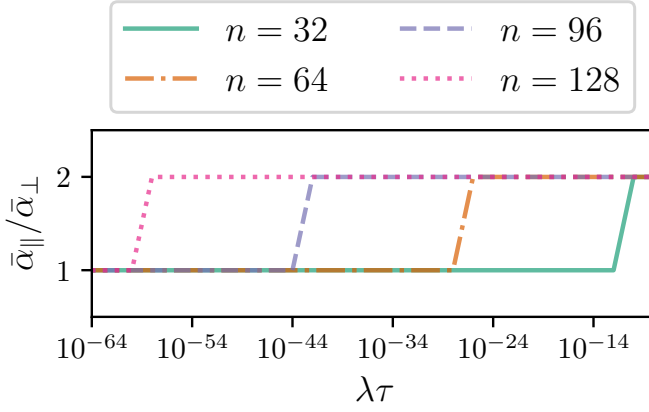


FIG. 4. Numerical evaluation of Gilbert damping anisotropy in the limit  $\lambda \rightarrow 0$ . Isotropic damping tensor is restored only if  $\lambda = 0$  with ultimate numerical precision. The factor of 2 anisotropy emerges at any finite  $\lambda$ , no matter how small it is, and only depends on the numerical precision  $n$ , i.e. the number of digits contained in each variable during computation. The crossover from isotropic to anisotropic damping can be understood only by considering finite, though vanishingly small, magnon  $q$  vectors.

factor of 2 anisotropy of Gilbert damping at  $\lambda = 0$ . We have seen above (see Fig. 4) that, surprisingly, there exists no energy scale for the anisotropy to emerge. The transition from the isotropic limit ( $\lambda = 0$ ) to a finite anisotropy appeared to take place exactly at  $\lambda = 0$ . We can, however, generalize the concept of Gilbert damping by considering the spin density response function at a finite wave vector  $\mathbf{q}$ .

To generalize the Gilbert damping, we are seeking a response of spin density at a point  $\mathbf{r}$ ,  $\delta\mathbf{s}_+(\mathbf{r})$  to a time derivative of magnetization vectors  $\dot{\mathbf{m}}_{\parallel}$  and  $\dot{\mathbf{m}}_{\perp}$  at the point  $\mathbf{r}'$ . The Fourier transform with respect to  $\mathbf{r} - \mathbf{r}'$  gives the Gilbert damping for a magnon with the wave-vector  $\mathbf{q}$ .

The generalization to a finite  $\mathbf{q}$ -vector shows that the limits  $\lambda \rightarrow 0$  and  $q \rightarrow 0$  cannot be interchanged. When the limit  $\lambda \rightarrow 0$  is taken before the limit  $q \rightarrow 0$  one finds an isotropic Gilbert damping, while for the opposite order of limits, it becomes a factor of 2 anisotropic. In a realistic situation, the value of  $q$  is limited from below by an inverse size of a typical magnetic domain  $1/L_m$ , while the spin-orbit coupling is effective on the length scale  $L_{\lambda} = 2\pi\hbar v_f/\lambda$ . In this picture, the isotropic Gilbert damping is characteristic for the case of sufficiently small domain size  $L_m \ll L_{\lambda}$ , while the anisotropic Gilbert damping corresponds to the case  $L_{\lambda} \ll L_m$ .

In the limit  $q\ell \ll 1$ , where  $\ell = v_f\tau$  is the electron mean

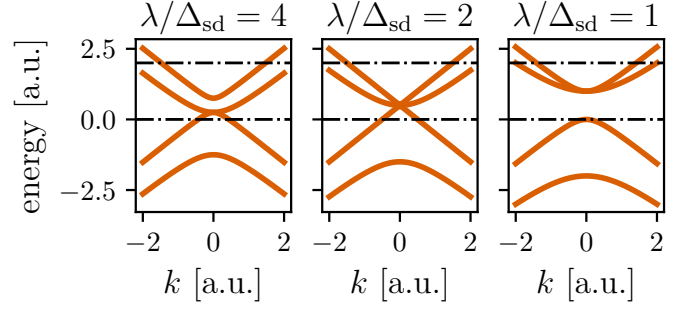


FIG. 5. Band-structure for the effective model of Eq. (5) in a vicinity of  $\mathbf{K}$  valley assuming  $n_z = 1$ . Electron bands touch for  $\lambda = 2\Delta_{sd}$ . The regime  $\lambda \leq 2\Delta_{sd}$  corresponds to spin-orbit band inversion. The band structure in the valley  $\mathbf{K}'$  is inverted. Our microscopic analysis is performed in the electron-doped regime for the Fermi energy above the gap as illustrated by the top dashed line. The bottom dashed line denotes zero energy (half-filling).

free path, we can summarize our results as

$$\bar{\alpha}_m^{\perp} = \varepsilon\tau \begin{cases} \frac{\varepsilon^2 + \Delta_{sd}^2}{2\Delta_{sd}^2} & \lambda\tau \ll q\ell \ll \Delta_{sd}/\varepsilon, \\ \frac{1}{3} \frac{\varepsilon^2 + \Delta_{sd}^2}{\Delta_{sd}^2} & q\ell \ll \lambda\tau \ll \Delta_{sd}/\varepsilon, \\ \frac{1}{2\lambda^2\tau^2} & \lambda\tau \gg \Delta_{sd}/\varepsilon, \end{cases} \quad (14a)$$

$$\bar{\alpha}_m^{\parallel} = \varepsilon\tau \begin{cases} \frac{\varepsilon^2 + \Delta_{sd}^2}{2\Delta_{sd}^2} & \lambda\tau \ll q\ell \ll \Delta_{sd}/\varepsilon, \\ \frac{2}{3} \frac{\varepsilon^2 + \Delta_{sd}^2}{\Delta_{sd}^2} & q\ell \ll \lambda\tau \ll \Delta_{sd}/\varepsilon, \\ 1 + \frac{1}{\lambda^2\tau^2} & \lambda\tau \gg \Delta_{sd}/\varepsilon, \end{cases} \quad (14b)$$

which represent a simple generalization of Eqs. (11).

The results of Eqs. (14) correspond to a simple behavior of Gilbert damping anisotropy,

$$\bar{\alpha}_m^{\parallel}/\bar{\alpha}_m^{\perp} = \begin{cases} 1 & \lambda\tau \ll q\ell, \\ 2(1 + \lambda^2\tau^2) & q\ell \ll \lambda\tau, \end{cases} \quad (15)$$

where we still assume  $q\ell \ll 1$ .

### III. ANTI-FERROMAGNETIC RESONANCE

The broadening of the anti-ferromagnet resonance peak is one obvious quantity that is sensitive to Gilbert damping. The broadening is however not solely defined by a particular Gilbert damping component but depends also on both magnetic anisotropy and anti-ferromagnetic exchange.

To be more consistent we can use the model of Eq. (5) to analyze the contribution of conduction electrons to an easy axis anisotropy. The latter is obtained by expanding the free energy for electrons in the value of  $n_z$ , which has a form  $E = -Kn_z^2/2$ . With the conditions  $\varepsilon/\lambda \gg 1$  and  $\varepsilon/\Delta_{sd} \gg 1$  we obtain the anisotropy constant as

$$K = \frac{\mathcal{A}}{2\pi\hbar^2v^2} \begin{cases} \Delta_{sd}^2\lambda & 2\Delta_{sd}/\lambda \leq 1, \\ \Delta_{sd}\lambda^2/2 & 2\Delta_{sd}/\lambda \geq 1, \end{cases} \quad (16)$$

where  $\mathcal{A}$  is the area of the unit cell. Here we assume both  $\lambda$  and  $\Delta_{\text{sd}}$  positive, therefore, the model naturally gives rise to an easy axis anisotropy with  $K > 0$ . In real materials, there exist other sources of easy axis or easy plane anisotropy. In-plane magneto-crystalline anisotropy also plays an important role. For example, Néel-type anti-ferromagnets with easy-axis anisotropy are  $\text{FePS}_3$ ,  $\text{FePSe}_3$  or  $\text{MnPS}_3$ , whereas those with easy plane and in-plane magneto-crystalline anisotropy are  $\text{NiPS}_3$  and  $\text{MnPSe}_3$ . Many of those materials are, however, Mott insulators. Our qualitative theory may still apply to materials like  $\text{MnPS}_3$  monolayers at strong electron doping.

The transition from  $2\Delta_{\text{sd}}/\lambda \geq 1$  to  $2\Delta_{\text{sd}}/\lambda \leq 1$  in Eq. (16) corresponds to the touching of two bands in the model of Eq. (5) as illustrated in Fig. 5.

Anti-ferromagnetic magnon frequency and life-time in the limit  $q \rightarrow 0$  are readily obtained by linearizing the equations of motion

$$\dot{\mathbf{n}} = -J\mathbf{n} \times \mathbf{m} + K\mathbf{m} \times \mathbf{n}_\perp + \mathbf{n} \times (\hat{\alpha}_m \dot{\mathbf{m}}), \quad (17a)$$

$$\dot{\mathbf{m}} = K\mathbf{n} \times \mathbf{n}_\perp + \mathbf{n} \times (\hat{\alpha}_n \dot{\mathbf{n}}), \quad (17b)$$

where we took into account easy axis anisotropy  $K$  and disregarded irrelevant terms  $\mathbf{m} \times (\hat{\alpha}_n \dot{\mathbf{n}})$  and  $\mathbf{m} \times (\hat{\alpha}_m \dot{\mathbf{m}})$ . We have also defined Gilbert damping tensors such as  $\hat{\alpha}_m \dot{\mathbf{m}} = \alpha_m^\parallel \dot{\mathbf{m}}_\parallel + \alpha_m^\perp \dot{\mathbf{m}}_\perp$ ,  $\hat{\alpha}_n \dot{\mathbf{n}} = \alpha_n^\parallel \dot{\mathbf{n}}_\parallel + \alpha_n^\perp \dot{\mathbf{n}}_\perp$ .

In the case of easy axis anisotropy we can use the linearized modes  $\mathbf{n} = \hat{\mathbf{z}} + \delta\mathbf{n}_\parallel e^{i\omega t}$ ,  $\mathbf{m} = \delta\mathbf{m}_\parallel e^{i\omega t}$ , hence we get the energy of  $q = 0$  magnon as

$$\omega = \omega_0 - i\Gamma/2, \quad (18)$$

$$\omega_0 = \sqrt{JK}, \quad \Gamma = J\alpha_n^\parallel + K\alpha_m^\parallel \quad (19)$$

where we took into account that  $K \ll J$ . The expression for  $\omega_0$  is well known due to Kittel and Keffer<sup>42,43</sup>.

Using Ref. 25 we find out that  $\alpha_n^\parallel \simeq \alpha_m^\perp (\lambda/\varepsilon)^2$  and  $\alpha_n^\perp \simeq \alpha_m^\parallel (\lambda/\varepsilon)^2$ , hence

$$\Gamma \simeq \alpha_m^\parallel \left( K + \frac{J/2}{\varepsilon^2/\lambda^2 + \varepsilon^2\tau^2} \right), \quad (20)$$

where we have simply used Eqs. (10). Thus, one may often ignore the contribution  $J\alpha_n^\parallel$  as compared to  $K\alpha_m^\parallel$  despite the fact that  $K \ll J$ .

In the context of anti-ferromagnets, spin-pumping terms are usually associated with the coefficients  $\alpha_n^\parallel$  in Eq. (3b) that are not in the focus of the present study. Those coefficients have been analyzed for example in Ref. 25. In this manuscript we simply use the known results for  $\alpha_n$  in Eqs. (17-19), where we illustrate the effect of both spin-pumping coefficient  $\alpha_n$  and the direct Gilbert damping  $\alpha_m$  on the magnon life time. One can see from Eqs. (19,20) that the spin-pumping contributions do also contribute, though indirectly, to the magnon decay. The spin pumping contributions become more important in magnetic materials with small magnetic anisotropy. The processes characterized by the coefficients  $\alpha_n$  may also be

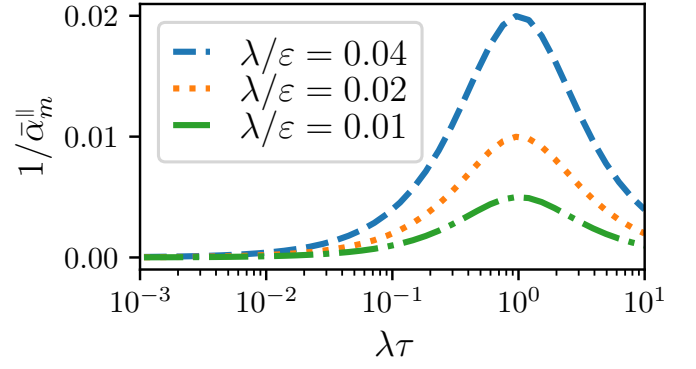


FIG. 6. Numerical evaluation of the inverse Gilbert damping  $1/\alpha_m^\parallel$  as a function of the momentum relaxation time  $\tau$ . The inverse damping is peaked at  $\tau \propto 1/\lambda$  which also corresponds to the maximum of the anti-ferromagnetic resonance quality factor in accordance with Eq. (21).

interpreted in terms of angular momentum transfer from one AFM sub-lattice to another. In that respect, the spin pumping is specific to AFM, and is qualitatively different from the direct Gilbert damping processes ( $\alpha_m$ ) that describe the direct momentum relaxation to the lattice.

As illustrated in Fig. 6 the quality factor of the anti-ferromagnetic resonance (for a metallic anti-ferromagnet with easy-axis anisotropy) is given by

$$Q = \frac{\omega_0}{\Gamma} \simeq \frac{1}{\alpha_m^\parallel} \sqrt{\frac{J}{K}}. \quad (21)$$

Interestingly, the quality factor defined by Eq. (21) is maximized for  $\lambda\tau \simeq 1$ , i.e. for the electron spin-orbit length being of the order of the scattering mean free path.

The quantities  $1/\sqrt{K}$  and  $1/\alpha_m^\parallel$  are illustrated in Fig. 6 from the numerical analysis. As one would expect, the quality factor vanishes in both limits  $\lambda \rightarrow 0$  and  $\lambda \rightarrow \infty$ . The former limit corresponds to an over-damped regime hence no resonance can be observed. The latter limit corresponds to a constant  $\alpha_m^\parallel$ , but the resonance width  $\Gamma$  grows faster with  $\lambda$  than  $\omega_0$  does, hence the vanishing quality factor.

It is straightforward to check that the results of Eqs. (20,21) remain consistent when considering systems with either easy-plane or in-plane magneto-crystalline anisotropy. Thus, the coefficient  $\alpha_m^\perp$  normally does not enter the magnon damping, unless the system is brought into a vicinity of spin-flop transition by a strong external field.

#### IV. CONCLUSION

In conclusion, we have analyzed the Gilbert damping tensor in a model of a two-dimensional anti-ferromagnet on a honeycomb lattice. We consider the damping mechanism that is dominated by a finite electron spin life-time

due to a combination of spin-orbit coupling and impurity scattering of conduction electrons. In the case of a 2D electron system with Rashba spin-orbit coupling  $\lambda$ , the Gilbert damping tensor is characterized by two components  $\alpha_m^\parallel$  and  $\alpha_m^\perp$ . We show that the anisotropy of Gilbert damping depends crucially on the parameter  $\lambda\tau$ , where  $\tau$  is the transport scattering time for conduction electrons. For  $\lambda\tau \ll 1$  the anisotropy is set by a geometric factor of 2,  $\alpha_m^\parallel = 2\alpha_m^\perp$ , while it becomes infinitely large in the opposite limit,  $\alpha_m^\parallel = (\lambda\tau)^2\alpha_m^\perp$  for  $\lambda\tau \gg 1$ . Gilbert damping becomes isotropic exactly for  $\lambda = 0$ , or, strictly speaking, for the case  $\lambda \ll \hbar v_f q$ , where  $q$  is the magnon wave vector.

This factor of 2 is essentially universal, and is a geometric effect: the z-component relaxation results from fluctuations in two in-plane spin components, whereas in-plane relaxation stems from fluctuations of the z-component alone. This reflects the subtleties of our microscopic model, where the mechanism for damping is activated by the decay of conduction electron momenta, linked to spin-relaxation through spin-orbit interactions.

We find that Gilbert damping is insensitive to magnetic order for  $\lambda \gg \Delta_{sd}/\varepsilon\tau$ , where  $\Delta_{sd}$  is an effective exchange coupling between spins of conduction and localized electrons. In this case, the electron spin relaxation can be either dominated by scattering (Dyakonov-Perel relaxation) or by spin-orbit precession (Elliot-Yafet relaxation). We find that the Gilbert damping component  $\alpha_m^\perp \simeq \varepsilon/\lambda^2\tau$  is dominated by Elliot-Yafet relaxation irrespective of the value of the parameter  $\lambda\tau$ , while the other component crosses over from  $\alpha_m^\parallel \simeq \varepsilon/\lambda^2\tau$  (Elliot-Yafet relaxation) for  $\lambda\tau \ll 1$ , to  $\alpha_m^\parallel \simeq \varepsilon\tau$  (Dyakonov-Perel relaxation) for  $\lambda\tau \gg 1$ . For the case  $\lambda \ll \Delta_{sd}/\varepsilon\tau$  the spin relaxation is dominated by interaction with the exchange field.

Crucially, our results are not confined solely to the Néel order on the honeycomb lattice: we anticipate a broader applicability across various magnetic orders, including the zigzag order. This universality stems from our focus on the large magnon wavelength limit. The choice of the honeycomb lattice arises from its unique ability to maintain isotropic electronic spectra within the plane, coupled with the ability to suppress anisotropy concerning in-plane spin rotations. Strong anisotropic electronic spectra would naturally induce strong anisotropic in-plane Gilbert damping, which are absent in our results.

Finally, we show that the anti-ferromagnetic resonance width is mostly defined by  $\alpha_m^\parallel$  and demonstrate that the resonance quality factor is maximized for  $\lambda\tau \approx 1$ . Our microscopic theory predictions may be tested for systems such as MnPS<sub>3</sub> monolayer on Pt and similar heterostructures.

## ACKNOWLEDGMENTS

We are grateful to O. Gomonay, R. Duine, J. Sinova, and A. Mauri for helpful discussions. This project has received funding from the European Union's Horizon 2020 research and innovation program under the Marie Skłodowska-Curie grant agreement No 873028.

## Appendix A: Microscopic framework

The microscopic model that we employ to calculate Gilbert damping belongs to a class of so-called *s-d* models that describe the physical system in the form of a Heisenberg model for localized spins and a tight-binding model for conduction electrons that are weakly coupled by a local magnetic exchange interaction of the strength  $\Delta_{sd}$ .

Our effective electron Hamiltonian for a metallic hexagonal anti-ferromagnet is given by<sup>25</sup>

$$H_0 = v_f \mathbf{p} \cdot \mathbf{\Sigma} + \frac{\lambda}{2} [\boldsymbol{\sigma} \times \mathbf{\Sigma}]_z - \Delta_{sd} \mathbf{n} \cdot \boldsymbol{\sigma} \Sigma_z \Lambda_z, \quad (\text{A1})$$

where the vectors  $\mathbf{\Sigma}$ ,  $\boldsymbol{\sigma}$  and  $\mathbf{\Lambda}$  denote the vectors of Pauli-matrices acting on sub-lattice, spin and valley space respectively. We also introduce the Fermi velocity  $v_f$ , Rashba-type spin-orbit interaction  $\lambda$ .

To describe Gilbert damping of the localized field  $\mathbf{n}$  we have to add the relaxation mechanism. This is provided in our model by adding a weak impurity potential  $H = H_0 + V(\mathbf{r})$ . The momentum relaxation due to scattering on impurities leads indirectly to the relaxation of Heisenberg spins due to the presence of spin-orbit coupling and exchange couplings.

For modeling the impurity potential, we adopt a delta-correlated random potential that corresponds to the point scatter approximation, where the range of the impurity potential is much shorter than that of the mean free path (see e.g. section 3.8 of Ref. 44), i.e.

$$\langle V(\mathbf{r})V(\mathbf{r}') \rangle = 2\pi\alpha(\hbar v_f)^2 \delta(\mathbf{r} - \mathbf{r}'), \quad (\text{A2})$$

where the dimensionless coefficient  $\alpha \ll 1$  characterizes the disorder strength. The corresponding scattering time for electrons is obtained as  $\tau = \hbar/\pi\alpha\varepsilon$ , which is again similar to the case of graphene.

The response of symmetric spin-polarization  $\delta s^+$  to the time-derivative of non-staggered magnetization,  $\partial_t \mathbf{m}$ , is defined by the linear relation

$$\delta s_\alpha^+ = \sum_\beta \mathcal{R}_{\alpha\beta}|_{\omega=0} \dot{m}_\beta, \quad (\text{A3})$$

where the response tensor is taken at zero frequency<sup>25,45</sup>. The linear response is defined generally by the tensor

$$\mathcal{R}_{\alpha\beta} = \frac{A\Delta_{sd}^2}{2\pi S} \int \frac{d\mathbf{p}}{(2\pi\hbar)^2} \langle \text{Tr} [C_{\varepsilon,\mathbf{p}}^R \sigma_\alpha G_{\varepsilon+\hbar\omega,\mathbf{p}}^A \sigma_\beta] \rangle, \quad (\text{A4})$$



where  $G_{\varepsilon, \mathbf{p}}^{\text{R(A)}}$  are standing for retarded(advanced) Green functions and the angular brackets denote averaging over disorder fluctuations.

The standard recipe for disorder averaging is the diffusive approximation<sup>46,47</sup> that is realized by replacing the bare Green functions in Eq. (A4) with disorder-averaged Green functions and by replacing one of the vertex operators  $\sigma_x$  or  $\sigma_y$  with the corresponding *vertex-corrected* operator that is formally obtained by summing up ladder impurity diagrams (diffusons).

In models with spin-orbit coupling, the controllable diffusive approximation for non-dissipative quantities may become, however, more involved as was noted first in Ref. 48. For Gilbert damping it is, however, sufficient to consider the ladder diagram contributions only.

The disorder-averaged Green function is obtained by including an imaginary part of the self-energy  $\Sigma^{\text{R}}$  (not to be confused here with the Pauli matrix  $\Sigma_{0,x,y,z}$ ) that is evaluated in the first Born approximation

$$\text{Im } \Sigma^{\text{R}} = 2\pi\alpha v_f^2 \int \frac{d\mathbf{p}}{(2\pi)^2} \text{Im} \frac{1}{\varepsilon - H_0 + i0}. \quad (\text{A5})$$

The real part of the self-energy leads to the renormalization of the energy scales  $\varepsilon$ ,  $\lambda$  and  $\Delta_{\text{sd}}$ .

In the first Born approximation, the disorder-averaged Green function is given by

$$G_{\varepsilon, \mathbf{p}}^{\text{R}} = \frac{1}{\varepsilon - H_0 - i \text{Im } \Sigma^{\text{R}}}. \quad (\text{A6})$$

The vertex corrections are computed in the diffusive approximation. The latter involves replacing the vertex  $\sigma_\alpha$  with the *vertex-corrected* operator,

$$\sigma_\alpha^{\text{vc}} = \sum_{l=0}^{\infty} \sigma_\alpha^{(l)}, \quad (\text{A7})$$

where the index  $l$  corresponds to the number of disorder lines in the ladder.

The operators  $\sigma_\alpha^{(l)}$  can be defined recursively as

$$\sigma_\alpha^{(l)} = \frac{2\hbar v_f^2}{\varepsilon\tau} \int \frac{d\mathbf{p}}{(2\pi)^2} G_{\varepsilon, \mathbf{p}}^{\text{R}} \sigma_\alpha^{(l-1)} G_{\varepsilon+\hbar\omega, \mathbf{p}}^{\text{A}}, \quad (\text{A8})$$

where  $\sigma_\alpha^{(0)} = \sigma_\alpha$ .

The summation in Eq. (A7) can be computed in the full operator basis,  $B_{i=\{\alpha, \beta, \gamma\}} = \sigma_\alpha \Sigma_\beta \Lambda_\gamma$ , where each index  $\alpha$ ,  $\beta$  and  $\gamma$  takes on 4 possible values (with zero standing for the unity matrix). We may always normalize  $\text{Tr } B_i B_j = 2\delta_{ij}$  in an analogy to the Pauli matrices. The operators  $B_i$  are, then, forming a finite-dimensional space for the recursion of Eq. (A8).

The vertex-corrected operators  $B_i^{\text{vc}}$  are obtained by summing up the matrix geometric series

$$B_i^{\text{vc}} = \sum_j \left( \frac{1}{1 - \mathcal{F}} \right)_{ij} B_j, \quad (\text{A9})$$

where the entities of the matrix  $\mathcal{F}$  are given by

$$\mathcal{F}_{ij} = \frac{\hbar v_f^2}{\varepsilon\tau} \int \frac{d\mathbf{p}}{(2\pi)^2} \text{Tr} [G_{\varepsilon, \mathbf{p}}^{\text{R}} B_i G_{\varepsilon+\hbar\omega, \mathbf{p}}^{\text{A}} B_j]. \quad (\text{A10})$$

Our operators of interest  $\sigma_x$  and  $\sigma_y$  can always be decomposed in the operator basis as

$$\sigma_\alpha = \frac{1}{2} \sum_i B_i \text{Tr}(\sigma_\alpha B_i), \quad (\text{A11})$$

hence the vertex-corrected spin operator is given by

$$\sigma_\alpha^{\text{vc}} = \frac{1}{2} \sum_{ij} B_i^{\text{vc}} \text{Tr}(\sigma_\alpha B_i). \quad (\text{A12})$$

Moreover, the computation of the entire response tensor of Eq. (A4) in the diffusive approximation can also be expressed via the matrix  $\mathcal{F}$  as

$$\mathcal{R}_{\alpha\beta} = \frac{\alpha_0 \varepsilon \tau}{8\hbar} \sum_{ij} [\text{Tr } \sigma_\alpha B_i] \left[ \frac{\mathcal{F}}{1 - \mathcal{F}} \right]_{ij} [\text{Tr } \sigma_\beta B_j], \quad (\text{A13})$$

where  $\alpha_0 = \mathcal{A} \Delta_{\text{sd}}^2 / \pi \hbar^2 v_f^2 S$  is the coefficient used in Eq. (6) to define the unit of the Gilbert damping.

It appears that one can always choose the basis of  $B_i$  operators such that the computation of Eq. (A13) is closed in a subspace of just three  $B_i$  operators with  $i = 1, 2, 3$ . This enables us to make analytical computations of Eq. (A13).

## Appendix B: Magnetization dynamics

The representation of the results can be made somewhat simpler by choosing  $x$  axis in the direction of the in-plane projection  $\mathbf{n}_\parallel$  of the Néel vector, hence  $n_y = 0$ . In this case, one can represent the result as

$$\delta \mathbf{s}^+ = c_1 \mathbf{n}_\parallel \times (\mathbf{n}_\parallel \times \partial_t \mathbf{m}_\parallel) + c_2 \partial_t \mathbf{m}_\parallel + c_3 \partial_t \mathbf{m}_\perp + c_4 \mathbf{n},$$

where  $\mathbf{n}$  dependence of the coefficients  $c_i$  may be parameterized as

$$c_1 = \frac{r_{11} - r_{22} - r_{31}(1 - n_z^2)/(n_x n_z)}{1 - n_z^2}, \quad (\text{B1a})$$

$$c_2 = r_{11} - r_{31}(1 - n_z^2)/(n_x n_z), \quad (\text{B1b})$$

$$c_3 = r_{33}, \quad (\text{B1c})$$

$$c_4 = (r_{31}/n_z) \partial_t m_z + \zeta(\partial_t \mathbf{m}) \cdot \mathbf{n}. \quad (\text{B1d})$$

The analytical results in the paper correspond to the evaluation of  $\delta \mathbf{s}^\pm$  up to the second order in  $\Delta_{\text{sd}}$  using perturbative analysis. Thus, zero approximation corresponds to setting  $\Delta_{\text{sd}} = 0$  in Eqs. (A1, A5).

The equations of motion on  $\mathbf{n}$  and  $\mathbf{m}$  are given by Eqs. (2),

$$\partial_t \mathbf{n} = -J \mathbf{n} \times \mathbf{m} + \mathbf{n} \times \delta \mathbf{s}^+ + \mathbf{m} \times \delta \mathbf{s}^-, \quad (\text{B2a})$$

$$\partial_t \mathbf{m} = \mathbf{m} \times \delta \mathbf{s}^+ + \mathbf{n} \times \delta \mathbf{s}^-, \quad (\text{B2b})$$

It is easy to see that the following transformation leaves the above equations invariant,

$$\delta \mathbf{s}^+ \rightarrow \delta \mathbf{s}^+ - \xi \mathbf{n}, \quad \delta \mathbf{s}^- \rightarrow \delta \mathbf{s}^- - \xi \mathbf{m}, \quad (\text{B3})$$

for an arbitrary value of  $\xi$ .

Such a gauge transformation can be used to prove that the coefficient  $c_4$  is irrelevant in Eqs. (B2).

In this paper, we compute  $\delta \mathbf{s}^\pm$  to the zeroth order in  $|\mathbf{m}|$  – the approximation which is justified by the sublattice symmetry in the anti-ferromagnet. A somewhat more general model has been analyzed also in Ref. 25 to which we refer the interested reader for more technical details.

### Appendix C: Anisotropy constant

The anisotropy constant is obtained from the grand potential energy  $\Omega$  for conducting electrons. For the model of Eq. (A1) the latter can be expressed as

$$\Omega = - \sum_{\varsigma=\pm} \frac{1}{\beta} \int d\varepsilon g(\varepsilon) \nu_{\varsigma}(\varepsilon), \quad (\text{C1})$$

where  $\beta = 1/k_B T$  is the inverse temperature,  $\varsigma = \pm$  is the valley index (for the valleys  $\mathbf{K}$  and  $\mathbf{K}'$ ),  $G_{\varsigma, \mathbf{p}}^R$  is the bare retarded Green function with momentum  $\mathbf{p}$  and in the valley  $\varsigma$ . We have also defined the function

$$g(\varepsilon) = \ln(1 + \exp[\beta(\mu - \varepsilon)]), \quad (\text{C2})$$

where  $\mu$  is the electron potential, and the electron density of states in each of the valleys is given by,

$$\nu_{\varsigma}(\varepsilon) = \frac{1}{\pi} \int \frac{d\mathbf{p}}{(2\pi\hbar)^2} \text{Im Tr } G_{\varsigma, \mathbf{p}}^R, \quad (\text{C3})$$

where the trace is taken only over spin and sub-lattice space,

In the metal regime considered, the chemical potential is assumed to be placed in the upper electronic band. In this case, the energy integration can be taken only for positive energies. The two valence bands are always filled and can only add a constant shift to the grand potential  $\Omega$  that we disregard.

The evaluation of Eq. (C1) yields the following density of states

$$\nu_{\tau}(\varepsilon) = \frac{1}{2\pi\hbar^2 v_f^2} \begin{cases} 0 & 0 < \varepsilon < \varepsilon_2 \\ \varepsilon/2 + \lambda/4 & \varepsilon_2 < \varepsilon < \varepsilon_1, \\ \varepsilon & \varepsilon > \varepsilon_1, \end{cases} \quad (\text{C4})$$

where the energies  $\varepsilon_{1,2}$  correspond to the extremum points (zero velocity) for the electronic bands. These energies, for each of the valleys, are given by

$$\varepsilon_{1,\varsigma} = \frac{1}{2} \left( +\lambda + \sqrt{4\Delta^2 + \lambda^2 - 4\varsigma\Delta\lambda n_z} \right), \quad (\text{C5a})$$

$$\varepsilon_{2,\varsigma} = \frac{1}{2} \left( -\lambda + \sqrt{4\Delta^2 + \lambda^2 + 4\varsigma\Delta\lambda n_z} \right) \quad (\text{C5b})$$

where  $\varsigma = \pm$  is the valley index.

In the limit of zero temperature we can approximate Eq. (C1) as

$$\Omega = - \sum_{\varsigma=\pm} \frac{1}{\beta} \int_0^\infty d\varepsilon (\mu - \varepsilon) \nu_{\varsigma}(\varepsilon). \quad (\text{C6})$$

Then, with the help of Eq. (C1) we find,

$$\Omega = - \frac{1}{24\pi\hbar^2 v_f^2} \sum_{\varsigma=\pm} [(\varepsilon_{1,\varsigma} - \mu)^2 (4\varepsilon_{1,\varsigma} - 3\lambda + 2\mu) + (\varepsilon_{2,\varsigma} - \mu)^2 (4\varepsilon_{2,\varsigma} + 3\lambda + 2\mu)]. \quad (\text{C7})$$

By substituting the results of Eqs. (C5) into the above equation we obtain

$$\Omega = - \frac{1}{24\pi\hbar^2 v_f^2} \left[ (4\Delta^2 - 4n_z\Delta\lambda + \lambda^2)^{2/3} + (4\Delta^2 + 4n_z\Delta\lambda + \lambda^2)^{2/3} - 24\Delta\mu + 8\mu^3 \right]. \quad (\text{C8})$$

A careful analysis shows that the minimal energy corresponds to  $n_z = \pm 1$  so that the conducting electrons prefer an easy-axis magnetic anisotropy. By expanding in powers of  $n_z^2$  around  $n_z = \pm 1$  we obtain  $\Omega = -Kn_z^2/2$ , where

$$K = \frac{1}{2\pi\hbar^2 v^2} \begin{cases} |\Delta^2 \lambda| & |\lambda/2\Delta| \geq 1, \\ |\Delta \lambda^2|/2 & |\lambda/2\Delta| \leq 1. \end{cases} \quad (\text{C9})$$

This provides us with the easy axis anisotropy of Eq. (16).

<sup>1</sup> S. A. Siddiqui, J. Sklenar, K. Kang, M. J. Gilbert, A. Schleife, N. Mason, and A. Hoffmann, Journal of Applied Physics **128**, 040904 (2020), [https://pubs.aip.org/aip/jap/article-](https://pubs.aip.org/aip/jap/article-pdf/doi/10.1063/5.0009445/15249168/040904_1_online.pdf)

[pdf/doi/10.1063/5.0009445/15249168/040904\\_1\\_online.pdf](https://pubs.aip.org/aip/jap/article-pdf/doi/10.1063/5.0009445/15249168/040904_1_online.pdf).  
<sup>2</sup> V. V. Mazurenko, Y. O. Kvashnin, A. I. Lichtenstein, and M. I. Katsnelson, Journal of Experimental and Theoretical Physics **132**, 506 (2021).

- <sup>3</sup> L. Šmejkal, J. Sinova, and T. Jungwirth, *Phys. Rev. X* **12**, 040501 (2022).
- <sup>4</sup> B. A. Bernevig, C. Felser, and H. Beidenkopf, *Nature* **603**, 41 (2022).
- <sup>5</sup> T. G. H. Blank, K. A. Grishunin, B. A. Ivanov, E. A. Mashkovich, D. Afanasiev, and A. V. Kimel, *Phys. Rev. Lett.* **131**, 096701 (2023).
- <sup>6</sup> W. Wu, C. Yaw Ameyaw, M. F. Doty, and M. B. Jungfleisch, *Journal of Applied Physics* **130**, 091101 (2021), <https://pubs.aip.org/aip/jap/article-pdf/doi/10.1063/5.0057536/13478272/091101.1.online.pdf>.
- <sup>7</sup> M. Gibertini, M. Koperski, A. F. Morpurgo, and K. S. Novoselov, *Nature Nanotechnology* **14**, 408 (2019).
- <sup>8</sup> K. M. D. Hals, Y. Tserkovnyak, and A. Brataas, *Physical Review Letters* **106**, 107206 (2011), publisher: American Physical Society.
- <sup>9</sup> R. Cheng, D. Xiao, and A. Brataas, *Physical Review Letters* **116**, 207603 (2016), publisher: American Physical Society.
- <sup>10</sup> S. Urazhdin and N. Anthony, *Physical Review Letters* **99**, 046602 (2007), publisher: American Physical Society.
- <sup>11</sup> R. Cheng, M. W. Daniels, J.-G. Zhu, and D. Xiao, *Physical Review B* **91**, 064423 (2015), publisher: American Physical Society.
- <sup>12</sup> R. Khymyn, I. Lisenkov, V. Tiberkevich, B. A. Ivanov, and A. Slavin, *Scientific Reports* **7**, 43705 (2017), number: 1 Publisher: Nature Publishing Group.
- <sup>13</sup> R. Cheng, J. Xiao, Q. Niu, and A. Brataas, *Physical Review Letters* **113**, 057601 (2014), publisher: American Physical Society.
- <sup>14</sup> A. Mougin, M. Cormier, J. P. Adam, P. J. Metaxas, and J. Ferré, *Europhysics Letters (EPL)* **78**, 57007 (2007), publisher: IOP Publishing.
- <sup>15</sup> A. A. Thiele, *Physical Review Letters* **30**, 230 (1973), publisher: American Physical Society.
- <sup>16</sup> R. Weber, D.-S. Han, I. Boventer, S. Jaiswal, R. Lebrun, G. Jakob, and M. Kläui, *Journal of Physics D: Applied Physics* **52**, 325001 (2019), publisher: IOP Publishing.
- <sup>17</sup> V. Y. Irkhin, A. A. Katanin, and M. I. Katsnelson, *Phys. Rev. B* **60**, 1082 (1999).
- <sup>18</sup> D. V. Spirin, *Journal of Magnetism and Magnetic Materials* **264**, 121 (2003).
- <sup>19</sup> J. Kosterlitz, *Journal of Physics C: Solid State Physics* **7**, 1046 (1974).
- <sup>20</sup> J. M. Kosterlitz and D. J. Thouless, in *Basic Notions Of Condensed Matter Physics* (CRC Press, 2018) pp. 493–515.
- <sup>21</sup> N. Mermin and H. Wagner, *Phys. Rev. Lett.* **17**, 1133 (1966).
- <sup>22</sup> B. L. Chittari, D. Lee, N. Banerjee, A. H. MacDonald, E. Hwang, and J. Jung, *Phys. Rev. B* **101**, 085415 (2020).
- <sup>23</sup> P. Högl, T. Frank, K. Zollner, D. Kochan, M. Gmitra, and J. Fabian, *Phys. Rev. Lett.* **124**, 136403 (2020).
- <sup>24</sup> K. Dolui, M. D. Petrović, K. Zollner, P. Plecháč, J. Fabian, and B. K. Nikolić, *Nano Lett.* **20**, 2288 (2020).
- <sup>25</sup> M. Baglai, R. J. Sokolewicz, A. Pervishko, M. I. Katsnelson, O. Eriksson, D. Yudin, and M. Titov, *Physical Review B* **101**, 104403 (2020), publisher: American Physical Society.
- <sup>26</sup> M. Fähnle and D. Steiauf, *Physical Review B* **73**, 184427 (2006).
- <sup>27</sup> H. T. Simensen, A. Kamra, R. E. Troncoso, and A. Brataas, *Physical Review B* **101**, 020403 (2020), publisher: American Physical Society.
- <sup>28</sup> A. Brataas, Y. Tserkovnyak, and G. E. W. Bauer, *Physical Review Letters* **101**, 037207 (2008), publisher: American Physical Society.
- <sup>29</sup> H. Ebert, S. Mankovsky, D. Ködderitzsch, and P. J. Kelly, *Physical Review Letters* **107**, 066603 (2011), publisher: American Physical Society.
- <sup>30</sup> Q. Liu, H. Y. Yuan, K. Xia, and Z. Yuan, *Physical Review Materials* **1**, 061401 (2017), publisher: American Physical Society.
- <sup>31</sup> M. Dyakonov and V. Perel, *Sov. Phys. Solid State, USSR* **13**, 3023 (1972).
- <sup>32</sup> M. Dyakonov and V. Kachorovskij, *Fizika i tehnika poluprovodnikov* **20**, 178 (1986).
- <sup>33</sup> R. Elliott, *Phys. Rev.* **96**, 266 (1954).
- <sup>34</sup> Y. Yafet, in *Solid State Physics*, Vol. 14, edited by F. Seitz and D. Turnbull (Elsevier, 1963) pp. 1–98.
- <sup>35</sup> M. Dyakonov, *arXiv:cond-mat/0401369* (2004).
- <sup>36</sup> M. I. Dyakonov, ed., *Spin Physics in Semiconductors*, 2nd ed., Springer Series in Solid-State Sciences (Springer International Publishing, 2017).
- <sup>37</sup> N. Averkiev, L. Golub, and M. Willander, *Semiconductors* **36**, 91 (2002).
- <sup>38</sup> A. Burkov, A. S. Núñez, and A. MacDonald, *Phys. Rev. B* **70**, 155308 (2004).
- <sup>39</sup> A. A. Burkov and L. Balents, *Physical Review B* **69**, 245312 (2004), publisher: American Physical Society.
- <sup>40</sup> N. A. Sinitsyn and Y. V. Pershin, *Reports on Progress in Physics* **79**, 106501 (2016), publisher: IOP Publishing.
- <sup>41</sup> A. Kamra, R. E. Troncoso, W. Belzig, and A. Brataas, *Phys. Rev. B* **98**, 184402 (2018).
- <sup>42</sup> C. Kittel, *Phys. Rev.* **82**, 565 (1951).
- <sup>43</sup> F. Keffer and C. Kittel, *Phys. Rev.* **85**, 329 (1952).
- <sup>44</sup> J. Rammer and H. Smith, *Rev. Mod. Phys.* **58**, 323 (1986).
- <sup>45</sup> I. Ado, O. A. Tretiakov, and M. Titov, *Phys. Rev. B* **95**, 094401 (2017).
- <sup>46</sup> J. Rammer, *Quantum Transport Theory* (CRC Press, New York, 2018).
- <sup>47</sup> G. D. Mahan, *Many-particle physics* (Springer Science & Business Media, 2013).
- <sup>48</sup> I. Ado, I. Dmitriev, P. Ostrovsky, and M. Titov, *EPL* **111**, 37004 (2015).